

MOL #43307

**A new mechanism of TAS-103 action discovered by target screening with drug-immobilized  
affinity beads**

**Makoto Yoshida, Yasuyuki Kabe, Tadashi Wada, Akira Asai, and**

**Hiroshi Handa**

**Graduate School of Bioscience and Biotechnology, Tokyo Institute of Technology, Yokohama**

**226-8501, Japan (M.Y.,Y.K.,T.W.,H.H.); Integrated Research Institute Graduate school of**

**Bioscience and Biotechnology, Tokyo Institute of Technology, Yokohama 226-8501, Japan**

**(T.W.,H.H.); Graduate School of pharmaceutical sciences, University of Shizuoka, Shizuoka**

**422-8526, Japan (A.A.)**

MOL #43307

Running title: TAS-103 disrupts signal recognition particle complex

Address correspondence to: Hiroshi Handa, Graduate School of Bioscience and Biotechnology, Tokyo

Institute of Technology, 4259 Nagatsuta-cho, Midori-ku, Yokohama, Kanagawa, 226-8501, Japan.

Tel: 81-45-924-5872; Fax: 81-45-924-5834 E-mail: [hhanda@bio.titech.ac.jp](mailto:hhanda@bio.titech.ac.jp)

The number of Text pages: 40

Tables: 0

Figures: 5

References: 34

The number of words in Abstract: 190

in Introduction: 665

in Discussion: 692

The abbreviations used are: SRP, signal recognition particle; DMF, N,N-dimethylformamide; SDS,

sodium dodecyl sulphate; PAGE, polyacrylamide gel electrophoresis; CBB, Coomassie Brilliant Blue;

IL-6, interleukin-6; topo, topoisomerase; NE, nuclear extract; NHS, N-hydroxysuccinimide; EDC,

N-ethyl-N'-(3-dimethylaminopropyl)-carbodiimide hydrochloride

MOL #43307

### **Abstract**

TAS-103 is a quinoline derivative that displays anti-tumour activity in murine and human tumour models. TAS-103 has been reported to be a potent topoisomerase II poison. However, other studies have indicated that cellular susceptibility to TAS-103 is not correlated with topoisomerase II expression. Since the direct target of TAS-103 remained unclear, we searched for a TAS-103 binding protein using high-performance affinity latex beads. We obtained a component of the signal recognition particle (SRP) as a TAS-103 binding protein. This component is a 54-kDa subunit (SRP54) of SRP, which mediates the proper delivery of secretory proteins in cells. We fractioned 293T cell lysates using gel-filtration chromatography and performed a co-immunoprecipitation assay using 293T cells expressing FLAG-tagged SRP54. The results revealed that TAS-103 disrupts SRP complex formation and reduces the amount of SRP14 and SRP19. RNAi-mediated knockdown of SRP54 or SRP14 promoted accumulation of the exogenously expressed chimeric protein, IL-6-FLAG, inside cells. In conclusion, we identified Signal Recognition particle as a target of TAS-103 by using affinity latex beads. This provides new insights into the mechanism underlying the effects of chemotherapies comprising TAS-103 and also demonstrates the usefulness of the affinity beads.

MOL #43307

## Introduction

Identifying proteins that bind specifically to drugs can help predict functions and estimate the efficacy of the drugs. It can also lead to novel drug development using computational designs based on information about drug-binding proteins.

We previously reported the application of the high-performance affinity latex beads, glycidylmethacrylate (GMA)-covered GMA–styrene copolymer core (SG beads), for identifying drug receptors (Shimizu et al., 2000; Tomohiro et al., 2002). These latex beads have several advantages over conventional affinity purification of receptors. They enable the rapid and efficient purification of ligand- or drug-binding proteins (Ohtsu et al., 2005). These high-performance affinity beads have been used successfully for purification of various proteins, including transcription factors and drug receptors (Shimizu et al., 2000; Uga et al., 2006) and cisplatin-damaged DNA-binding proteins (Tomohiro et al., 2002).

TAS-103 has been developed as an anticancer drug and displays antitumour activity in murine and human tumour models. It is a potent dual-inhibitor of topoisomerases (topo) I and II

MOL #43307

(Azuma and Urakawa, 1997; Utsugi et al., 1997), the enzymes associated with cleavage, passage, and recombination of DNA during DNA and RNA synthesis (Osheroff, 1989a; Wang, 1985), and exhibits powerful and broad anti-tumour activity against subcutaneously implanted human solid tumour xenografts, including cancers of the lung, colon, stomach, breast, pancreas, and kidney (Schabel et al., 1979). Its topo I inhibitory activity is similar to that of SN-38, and its topo II inhibitory activity is stronger than that of the inhibitor VP-16 (Sunami et al., 1999; Utsugi et al., 1997). TAS-103 does not show any cross-resistance in several resistant phenotypes such as cis-diamminedichloroplatinum(II) resistance, multi-drug resistance, or topoisomerase inhibitor resistance (Sunami et al., 1999). It also enhances DNA cleavage *in vitro* in the presence of mammalian topo I and human topo II $\alpha$  and II $\beta$ . However, a study in yeast concluded that topo II is a primary cellular target of TAS-103 (Byl et al., 1999).

Although the levels of topo II expression have been shown to correlate with the sensitivity of cancer cells to topo II poisons (Takano et al., 1992), another study has shown that cellular susceptibility to TAS-103 is not correlated with topo II expression and is correlated with p300 expression (Torigoe et al., 2005). p300 functions together with Sp1 in GC-box-dependent transcription

MOL #43307

(Suzuki et al., 2000; Xiao et al., 2000). That study has also demonstrated that TAS-103 treatment enhances the interaction of Sp1 with p300 and induces SV40 promoter activity in a GC-box-dependent manner in cells in which p300 is highly expressed (Torigoe et al., 2005). Nevertheless, the direct target of TAS-103 has remained unclear. Therefore, we have searched for another target protein of TAS-103 using the high-performance affinity latex beads and have identified a component of the signal recognition particle (SRP) as a TAS-103 binding protein.

The SRP is a ribonucleoprotein complex composed of an Alu domain and an S domain in mammalian cells. The Alu domain contains two SRP proteins: SRP9 and SRP14. The S domain contains unique sequence SRP RNA and four SRP proteins: SRP19, SRP54, SRP68, and SRP72 (Politz et al., 2000). The SRP is bound through SRP54 to the signal peptides of membrane and secretory proteins emerging from the ribosome. Following signal peptide recognition, the SRP is bound to membrane receptors to ensure the proper delivery of secretory proteins (Keenan et al., 2001; Lutcke, 1995; Rosenblad et al., 2003; Zwieb and Eichler, 2002). Low levels of SRP lead to insufficient targeting of proteins to the ER (Lakkaraju et al., 2007).

MOL #43307

Here we show that TAS-103 is not only bound to SRP54, but also disrupts SRP complex formation and reduces the amount of the SRP14 subunit. We have employed interleukin-6 (IL-6)-FLAG as a model secretory protein with a signal peptide. TAS-103 treatment increases the level of intracellular IL-6-FLAG protein, similar to RNAi-mediated knockdown of SRP54 or SRP14. We propose that TAS-103 disrupts SRP complex formation and causes degradation of SRP14 through its binding to SRP54. As a result, TAS-103 inhibits the function of the SRP in directing the delivery of secretory proteins.

MOL #43307

## Materials and Methods

**TAS-103 immobilization to latex beads.** The TAS-103 derivative TAS-1-3383 (Fig. 1B) were fixed to latex beads (SGNGDENC beads) as previously described ((Shima et al., 2003), Fig. 1C). The TAS-1-3383 was synthesized by Taiho Pharmaceutical Co., Ltd. and was dissolved at 1 mM in N,N-dimethylformamide (DMF; Nacalai Tesque, Kyoto, Japan) containing 9 mM triethylamine, followed by diluting to 0.3 mM and 0.1 mM with DMF containing 9 mM triethylamine. The SGNGDENC beads (5 mg) were reacted with 0.2mM N-hydroxysuccinimide (NHS) and 0.2mM N-ethyl-N'-(3-dimethylaminopropyl)-carbodiimide hydrochloride (EDC), and then mixed with 500  $\mu$ l of the 1.0-mM, 0.3-mM, and 0.1-mM TAS-1-3383 solutions for 16 hours at room temperature. After removal of the supernatants to fresh tubes, 500  $\mu$ l of 1 M ethanolamine (pH 8.5) were added to the beads and mixed for 2 hours to block unreacted amino groups on the beads. The concentrations of residual NHS in the supernatants were measured by high-performance liquid chromatography (HPLC) to quantify the immobilized TAS-1-3383.

**Cell cultures.** HeLa spinner cells were grown in MEM medium containing 10% horse serum



MOL #43307

as described previously (Wada et al., 1991). HeLa and 293T cells were cultured in DMEM medium (Invitrogen, San Diego, CA) supplemented with 10% fetal bovine serum, 50 U/ml penicillin, and 50 g/ml streptomycin. Cells were cultured at 37°C under an atmosphere of 5% CO<sub>2</sub>.

***Preparation of HeLa cell extracts.*** Nuclear extracts (NE) of HeLa cells were prepared as previously described (Dignam et al., 1983; Ohtsu et al., 2005; Wada et al., 1998). The extracts were dialyzed against buffer E (10 mM Tris-HCl, 50 mM NaCl, 1 mM MgCl<sub>2</sub>, 1 mM CaCl<sub>2</sub>, 0.2 mM EDTA, 10% glycerol) without NP-40.

***Affinity purification of drug-binding proteins.*** TAS-1-3383-fixed latex beads (0.3 mg) were equilibrated with buffer E, mixed with 200 µl of NE, incubated at 4°C for 4 hours with occasional agitation, washed with buffer E three times, and then agitated in 50 µl of buffer E containing 10 mM TAS-103 at 4°C for 1 hour to elute the binding protein(s). The protein was visualized by silver staining and Coomassie Brilliant Blue (CBB) staining. CBB-stained bands were subjected to in-gel trypsin digestion, and the resultant peptides were analysed by liquid chromatography mass spectrometry (LC-MS).

MOL #43307

**RNase treatment.** Molecular biology grade RNase A solution (5  $\mu$ l) (USB Corporation, Cleveland, OH) was added to the extracts before affinity purification.

**Western blotting.** Total protein was quantified using a Bradford protein assay (Bio-Rad, Hercules, CA). Equal amounts of protein were loaded into sodium dodecyl sulphate (SDS)-polyacrylamide gels and transferred to PVDF filters (Millipore, Bedford, MA). Filters were blocked in blocking buffer (20 mM Tris-HCl, pH 7.6, 150 mM NaCl, 10% NaN<sub>3</sub>, and 3% BSA) and washed in TBS-T (20 mM Tris-HCl, pH 7.6, 150 mM NaCl, 0.1% Tween 20). The primary antibodies were anti- $\beta$ -actin (Chemicon, Temecula, CA), anti-SRP54 (BD Biosciences Pharmingen, San Diego, CA), anti-SRP14 (Santa Cruz Biotechnology, Santa Cruz, CA), anti-FLAG (Sigma-Aldrich, St. Louis, MO), anti-SRP19, kindly provided by Dirk Görlich (Zentrum für Molekulare Biologie der Universität Heidelberg, Heidelberg, Germany) (Dean et al., 2001), and anti-SRP72-4 and anti-SRP68-2, kindly provided by Bernhard Dobberstein (Zentrum für Molekulare Biologie der Universität Heidelberg) (Bacher et al., 1999; Lutcke et al., 1993). The secondary antibodies conjugated to horseradish peroxidase were anti-mouse IgG (Sigma-Aldrich), anti-goat IgG (Santa Cruz Biotechnology), and anti-rabbit IgG (Cell Signaling Technology, Danvers, MA). Signals were detected using the ECL

MOL #43307

system (GE Healthcare, Pittsburgh, PA) and Kodak Biomax films (Eastman Kodak, Rochester, NY)

***Gel-filtration studies.*** The formation of the SRP was studied by gel-filtration chromatography using a SMART system and a Superose-6 PC 3.2/30 column (GE Healthcare). 293T cells were seeded into 60-mm collagen-coated dishes at  $10 \times 10^5$  cells per dish. TAS-103 was added when the cultures had reached approximately 70–80% confluence. The cells were cultured for the next 12 hours in the presence or absence of 10  $\mu$ M TAS-103, collected with a scraper in PBS, washed with ice-cold PBS, lysed in 400  $\mu$ l of 0.5% NP-40 lysis buffer (50 mM Tris-HCl, pH 8, 100 mM NaCl, and 0.5% NP-40) with occasional agitation, and centrifuged at  $16,000 \times g$  for 20 minutes at  $4^\circ\text{C}$  to remove any insoluble material. The supernatants were filtered with a 0.22- $\mu$ m filter unit. The supernatants (50  $\mu$ l) were loaded on the Superose-6 column equilibrated with the 0.5% NP-40 lysis buffer and collected fractions were analysed by western blotting using antibodies against SRP54, SRP72, SRP68, and  $\beta$ -actin as a control. Molecular mass standards consisting of BSA (66 kDa), alcohol dehydrogenase (150 kDa), horse spleen apoferritin (443 kDa), and bovine thyroglobulin (669 kDa) were used for calibration.

MOL #43307

**Construction of the FLAG-tagged IL-6 plasmid.** A DNA insert encoding the FLAG-tagged human IL-6 fusion protein was constructed by polymerase chain reaction using the *IL-6* cDNA and the primers 5'-GATGATATCGAATTCATGAACTCCTTCTCCACAAGCG-3' and 5'-GAGGATATCC TCGAGGACTCAGTCACTTAACTTGTCGTCATCCTTGTAGTCCATCATTGCGGAAGAGCCC TCAG-3', followed by treatment with *EcoR* I and *Xho* I, and inserted into the expression vector pcDNA3.1 (Invitrogen) between the *EcoR* I and *Xho* I sites.

**Construction of the FLAG-tagged IL-6 plasmid lacking a signal peptide.** A DNA insert encoding the FLAG-tagged human IL-6 fusion protein was constructed by PCR using the *IL-6* cDNA and the primers 5'- GATGATATCGAATTCATGGCCCCAGTACCCCCAGGA-3' and 5'-GAGGATATCCTCGAGGACTCAGTCACTTAACTTGTCGTCATCCTTGTAGTCCATCATT GCCGAAGAGCCCTCAG-3', followed by treatment with *Eco* RI and *Xho* I, and inserted into the expression vector pcDNA3.1 between the *EcoR* I and *Xho* I sites.

**Immunoprecipitation.** 293T cells were washed with ice-cold PBS, lysed in 250  $\mu$ l of the 0.5% NP-40 lysis buffer with occasional agitation, and centrifuged at 16,000 $\times$ g for 10 minutes at 4°C

MOL #43307

to remove any insoluble material. ANTI-FLAG<sup>®</sup> M2 Affinity Gel (Sigma) was equilibrated in the 0.5% NP-40 lysis buffer. The supernatant (200  $\mu$ l) was transferred to a fresh tube containing 20  $\mu$ l of the equilibrated packed gel and incubated at 4°C with rotation for 3 hours. The beads were collected by centrifugation at 500 $\times$ g for 5 minutes and washed 3 times with 1 ml of 0.5% NP-40 lysis buffer. The FLAG-tagged protein was competitively eluted with 50  $\mu$ l of 0.5% NP-40 lysis buffer containing 0.2  $\mu$ g/ $\mu$ l FLAG peptides.

***Co-immunoprecipitation assay.*** 293T cells were seeded into 60-mm collagen-coated dishes at  $10 \times 10^5$  cells per dish. After 12 hours, the cells were transfected with the plasmid pcDNA3-FLAG-HIS-SRP54. At 12 hours after transfection, the medium was changed. TAS-103 was added when the cultures achieved approximately 70–80% confluence. The cells were cultured for the next 12 hours in the presence or absence of 10  $\mu$ M TAS-103, collected with a scraper in PBS, and washed with ice-cold PBS. The cells were lysed in 400  $\mu$ l of 0.5% NP-40 lysis buffer with occasional agitation and centrifuged at 16,000 $\times$ g for 20 minutes at 4°C to remove any insoluble material. RNase A solution (5  $\mu$ l) was added to the lysate before immunoprecipitation. The cell lysate (300  $\mu$ l) was immunoprecipitated using ANTI-FLAG<sup>®</sup>-M2 agarose beads (Sigma). The eluted fraction and the

MOL #43307

whole-cell lysate were analysed by western blotting with anti-SRP54, anti-SRP68, anti-SRP72, anti-SRP19, anti-SRP14, and anti- $\beta$ -actin.

*Analysis of the effects of RNAi-mediated knockdown of SRP54 or SRP14 on the delivery of IL-6-FLAG.* 293T cells were seeded into 60-mm collagen-coated dishes at  $10 \times 10^5$  cells per dish. After 24 hours the cells were transfected with the plasmids pcDNA3.1-IL-6-FLAG or pcDNA3.1-IL-6 $\Delta$ S-FLAG and the stealth RNAs (Invitrogen) using lipofectamine 2000 (Invitrogen). The medium was changed 12 hours later. After another 12 hours, one-half of the cells was passaged in one plate and incubated for 24 hours. The cells and culture media were collected at 48 hours after transfection. The lysates were immunoprecipitated and analyzed by western blotting. The sequences of the stealth RNAs were as follows: stealth RNA targeting SRP54, sense 5'-GGATCCTGTCATCATT GCTTCTGAA-3'; stealth RNA targeting SRP14: sense 5'-GCTAACATGGATGGGCTGAAGAAG A-3'.

*Analysis of the effects of TAS-103 on the translocation of IL-6-FLAG.* 293T cells were transfected with pcDNA3.1-IL-6-FLAG or pcDNA3.1-IL-6 $\Delta$ S-FLAG and the medium was changed

MOL #43307

after 16 hours. The cells were cultured for another 8 hours in the presence or absence of TAS-103. The

cells and culture media were collected at 24 hours after transfection.

MOL #43307

## Results

### The SRP binds to TAS-103

TAS-103 is an anticancer drug that likely exerts its effect on tumour cell viability by inhibiting topoisomerase activity (Azuma and Urakawa, 1997; Byl et al., 1999; Fortune et al., 1999; Ishida and Asao, 1999; Osheroff, 1989a; Utsugi et al., 1997; Wang, 1985). However, other studies have indicated that cellular susceptibility to TAS-103 is not correlated with topo II expression (Torigoe et al., 2005). Since the direct target of TAS-103 remained unclear, we searched for other TAS-103 binding protein(s) in HeLa cell extracts using the high-performance affinity latex beads carrying a TAS-103 derivative, TAS-1-3383, which has an additional amino group for the coupling reaction with the carboxyl groups of the beads ((Ohtsu et al., 2005; Shimizu et al., 2000); Fig. 1B).

We examined the biological activity of TAS-1-3383 before its immobilization on the beads. Cell viability assays were performed on HeLa cells cultured with TAS-103 or TAS-1-3383. The  $IC_{50}$  values were 40 nM and 500 nM for the cells cultured with TAS-103 and TAS-1-3383, respectively (data not shown). This result indicated that the additional amino group of TAS-1-3383 reduced its



MOL #43307

cytotoxicity on HeLa cells, but that TAS-1-3383 still had a negative effect on tumour cell viability.

TAS-1-3383 was immobilized as shown in Figure 1C. Three different concentrations of TAS-1-3383 in DMF were incubated with the latex beads, and the amounts of TAS-1-3383 immobilized on the surface of the beads were calculated as described in the Material and Methods. The concentrations of TAS-1-3383 were 1.1 nmol/mg, 2.1 nmol/mg, and 4.8 nmol/mg. Control beads without the TAS-103 derivative were also employed. HeLa cell nuclear extracts were incubated with each of the beads for 12 hours. The beads with bound proteins were washed three times and then the proteins were recovered from the beads in the presence of 10 mM TAS-103. The proteins were subjected to SDS-polyacrylamide gel electrophoresis (PAGE) and visualized by silver staining. We observed several bands in all lanes; however, a single band with a molecular mass of 54 kDa was detected only in lanes containing material from the TAS-1-3383-immobilized beads (Fig. 2A). Furthermore, the band intensity increased with increasing concentrations of TAS-1-3383 on the beads (Fig. 2A). These results indicate that the 54-kDa band is specific for the immobilized TAS-1-3383.

We analysed the 54-kDa protein by LC-MS and found that it might be SRP54, a component

MOL #43307

of the SRP. To test whether the 54-kDa band was SRP54, we carried out western blot analysis with anti-SRP54 antibody. The antibody reacted with the 54-kDa protein and the band intensity increased in proportion to the amount of TAS-1-3383 immobilized on the beads (Fig. 2B). These results indicate that SRP54 was specifically bound to TAS-1-3383 on beads and was eluted competitively by the addition of TAS-103.

#### **TAS-103 disrupts SRP complex formation**

We investigated whether TAS-103 affects SRP complex formation. We chose 293T cells for this assay because 293T whole-cell lysates can be readily prepared under mild detergent conditions. The 293T cells were incubated for 12 hours with or without 10  $\mu$ M TAS-103 and lysed in lysis buffer containing 0.5% NP-40. The cell extracts were fractionated by gel-filtration chromatography as described in the Materials and Methods. Each fraction was analysed by western blotting with anti-SRP54, anti-SRP68, anti-SRP72, and anti- $\beta$ -actin antibodies (see Materials and Methods for experimental details). SRP68 and SRP72 were observed in fractions 7, 8, and 9 regardless of TAS-103 treatment. In contrast, SRP54 was observed primarily in fractions 8-11 of cells cultured without

MOL #43307

TAS-103, whereas it was observed in fractions 8-12, and abundantly in fractions 11 and 12, of cells cultured with TAS-103, indicating that the addition of TAS-103 caused SRP54 to distribute in later fractions (Fig. 3A). TAS-103 treatment did not affect the distribution of  $\beta$ -actin, which was detected in fractions 11-14. The band intensities of the SRP54 and  $\beta$ -actin proteins were measured using the NIH Image-J freeware program (<http://rsb.info.nih.gov/ij/>) and plotted in Figure 3B, which shows the clear difference in SRP54 distribution with TAS-103 treatment (Fig. 3B, left). In contrast, the control  $\beta$ -actin distribution was similar in fractions 10-14 regardless of the treatment (Fig. 3B, right). These results indicate that TAS-103 releases SRP54 from SRP68 and SRP72.

To better understand the effects of TAS-103 on the interactions between SRP54 and other subunits, we performed a co-immunoprecipitation assay. We over-expressed FLAG-tagged SRP54 in 293T cells. Untreated 293T cells were used as a control. The 293T cells were incubated for 12 hours with or without 10  $\mu$ M TAS-103 and lysed in lysis buffer containing 0.5% NP-40. The over-expressed FLAG-tagged SRP54 was immunoprecipitated using ANTI-FLAG<sup>®</sup>-M2 agarose beads and released from the beads using FLAG peptide. The eluates were analyzed by western blotting with anti-SRP54, anti-SRP68, anti-SRP72, anti-SRP19, anti-SRP14, and anti- $\beta$ -actin antibodies (Fig. 4A). These SRP

MOL #43307

subunits were detected in the eluates from the 293T cells over-expressing SRP54-FLAG (Fig. 4A, lanes 2 and 4), whereas no bands were detected in the eluates from control cells (Fig. 4A, lanes 1 and 3). The band intensities of SRP68 and SRP72 were decreased in the eluates from cells grown with TAS-103 (Fig. 4A, compare lanes 2 and 4). These data indicate that SRP68 and SRP72 are released from SRP54 by the addition of TAS-103, consistent with the results of the gel-filtration assay shown in Figure 3.

Furthermore, the band intensities of SRP14 and SRP19 were decreased in the whole-cell lysates from cells treated with TAS-103 (Fig. 4A, compare lanes 7 and 9 and lanes 8 and 10, respectively). The decreases were dose dependent (Fig. 4B). However, SRP14 mRNA was unaffected by treatment with TAS-103 (data not shown). These results suggest that TAS-103 causes the disruption of the SRP complex, resulting in destabilization of SRP14 and SRP19 and its eventual degradation. Further in-depth studies will be required to elucidate the mechanism in detail.

**TAS-103 treatment and the knockdown of SRP54 and SRP14 cause an intracellular increase in IL-6-FLAG**

MOL #43307

The SRP interacts with signal sequences that appear on the surface of translating ribosomes. Following signal-peptide recognition, the SRP is bound to membrane receptors and ensures the proper delivery of secretory proteins (Keenan et al., 2001; Lutcke, 1995; Rosenblad et al., 2003; Zwieb and Eichler, 2002). We hypothesized that TAS-103 inhibits the translocation of proteins into the ER, thereby leading to the inhibition of translocation across the ER and resulting in the accumulation of secretory proteins in the cells.

IL-6 is a multifunctional cytokine that is produced by many cells following appropriate stimulation. IL-6 has a signal peptide for sorting and directing it to the ER via the SRP during translation. IL-6 lacking the signal peptide accumulates within the cytoplasm of transfected cells (Rose-John et al., 1993). Therefore, to examine whether TAS-103 causes secretory proteins with signal peptides to accumulate in cells, we employed IL-6-FLAG with its signal peptide as a model and IL-6-FLAG lacking the signal peptide (IL-6 $\Delta$ S-FLAG) as a negative control.

293T cells were transfected with pcDNA3.1-IL6-FLAG or pcDNA3.1-IL6 $\Delta$ S-FLAG and cultured for 12 hours. After a medium change, the cells were incubated with or without TAS-103 for

MOL #43307

another 8 hours. The cell lysates and culture media were immunoprecipitated by anti-FLAG antibody, followed by western blot analysis. The results showed that TAS-103 caused an increase in IL-6-FLAG in the cell lysates (Fig. 5A), but had no effect on the accumulation of IL6 $\Delta$ S-FLAG (Fig. 5B).

To test whether specific reductions in SRP54 or SRP14 protein affected the accumulation of IL-6-FLAG or IL6 $\Delta$ S-FLAG in cells, we performed RNAi-mediated knockdowns of SRP54 and SRP14. The cells were co-transfected with the pcDNA3.1-IL6-FLAG plasmid or -IL6 $\Delta$ S-FLAG plasmid and stealth RNA targeting SRP14 or SRP54 or control stealth RNA containing a scrambled sequence. The cell lysates and culture media were immunoprecipitated followed by western blot analysis. The specific knockdowns of SRP54 and SRP14 were confirmed by western blot analysis (Fig. 5C). The results showed that the reductions in SRP54 or SRP14 proteins increased intracellular IL-6-FLAG as compared with the treatment with stealth RNA containing the scrambled sequence (Fig. 5C). In contrast, in cells co-transfected with the pcDNA3.1-IL6 $\Delta$ S-FLAG plasmid and the stealth RNAs, the reductions in SRP54 or SRP14 protein had no effect on the amount of intracellular IL6 $\Delta$ S-FLAG (Fig. 5D). Thus, treatment with TAS-103 and the specific knockdowns of SRP54 or SRP14 had similar effects on the accumulation of intracellular IL6-FLAG.

MOL #43307

These results suggest that TAS-103 treatment causes the accumulation of intracellular IL-6-FLAG by inhibiting the SRP and thereby disrupting proper protein delivery.

MOL #43307

## Discussion

We have identified SRP54 as a protein associated with TAS-103 using affinity latex beads.

The addition of TAS-103 dissociates SRP54 from TAS-1-3383 immobilized to the latex beads.

Although SRP54 has been reported to be localized in the cytosol (Politz et al., 2000), we observe abundant SRP54 in HeLa cell nuclear extracts (Fig. 2B). Because DNA also has been considered to be a major target of TAS-103 (Ishida and Asao, 1999), we predicted that TAS-103 bound to SRP54 via nucleic acid. However, SRP54 was bound to the drug in the lysates treated with RNaseA (Fig. 2C) and the co-immunoprecipitation assay using FLAG-tagged SRP54 showed that SRP14 was released by the RNaseA treatment (Fig. 4A). We, therefore, deduce that SRP54 is a TAS-103-binding protein.

TAS-103 is classified as a topo II poison (Byl et al., 1999). Nevertheless, we did not find any topo II associated with TAS-103 (data not shown). We investigated TAS-103 binding proteins from the NE lysate lacking abundant supercoiled DNA, whereas TAS-103 stabilizes the covalently linked topo II-DNA complex called the “cleavable complex” (Willmore et al., 1998). In the drug-stabilized cleavable complex, topo II molecules are covalently bound to a DNA strand end at the double-strand



MOL #43307

break, thereby preventing re-ligation of the DNA strands (Osheroff, 1989b). These stabilized complexes are believed to make the break permanent and inhibit DNA replication, leading to mutations, recombination events, and chromosome aberrations (Chen et al., 1996). We obtained a TAS-103 binding protein from NE lysates that did not contain abundant supercoiled DNA, whereas TAS-103 likely recognizes topoisomerases bound to supercoiled double-stranded DNA in cells. This may be a reason why topoisomerases were not obtained from the beads in our study, although further in-depth studies will be required to address this question.

We have shown that TAS-103 disrupts SRP complex formation and decreases the amounts of SRP14 and SRP19 in cells. SRP14 mRNA was not affected by addition of TAS-103. Therefore, these results suggest that TAS-103 destabilizes SRP14 and SRP19 through the disruption of the SRP complex.

The SRP interacts with signal sequences appearing on the surface of translating ribosomes, followed by binding to membrane receptors to ensure the proper delivery of secretory proteins (Lutcke, 1995; Rosenblad et al., 2003; Zwieb and Eichler, 2002). We have employed IL-6-FLAG as a model

MOL #43307

protein with a signal peptide that is delivered by the SRP and IL-6-FLAG lacking a signal peptide (IL-6 $\Delta$ S-FLAG) as a negative control. We have examined the effects of TAS-103 and knockdowns of SRP54 and SRP14 on the translocation of IL-6-FLAG and IL-6 $\Delta$ S-FLAG and found that they increase intracellular IL-6-FLAG, whereas they have no effect on the amount of IL-6 $\Delta$ S-FLAG. Therefore, we hypothesize that the accumulation is caused by disruption of post-translational translocation. We have observed that the addition of TAS-103 or RNAi-mediated knockdowns lead to increases in two types of intracellular IL-6-FLAG with different molecular weights. The reason for this is unknown; however, the increase in the molecular weight of the intracellular IL-6-FLAG was the same with the TAS-103 treatment as with the knockdowns.

Although we observed the accumulation of IL-6-FLAG caused by RNAi-mediated knockdowns of SRP14 or SRP54 or TAS-103 treatment, no corresponding decrease of IL-6-FLAG in the culture media was detected. The amount of IL-6-FLAG secreted from 293T cells into the culture media was found to be 20-40-fold more than the amount inside the cells (data not shown). The amount of intracellular IL-6-FLAG in cells treated with TAS-103 was two-four times more than in untreated cells. We speculate that the difference in the amount of IL-6-FLAG secreted into the culture media by

MOL #43307

TAS-103-treated and untreated cells was very small and therefore undetectable by western blot analysis.

From these observations, we propose that the interaction between SRP and TAS-103 results in disruption of SRP complex formation and degradation of SRP14 and 19, and eventually inhibiting SRP function. This provides new insights into the mechanism underlying the effects of chemotherapies comprising TAS-103.

Nowadays, various chemical genetic approaches for the probing of potential interactions between large numbers of chemical compounds and potential targets are being actively explored for drug discovery. This work describes the usefulness of our affinity beads for providing high quality chemical genetic information.

MOL #43307

### **Acknowledgements**

The authors would like to thank Prof. Bernhard Dobberstein and Prof. Dirk Görlich (Zentrum für Molekulare Biologie der Universität Heidelberg, Heidelberg, Germany) for providing the antibodies, Shinji Okazaki (Taiho Pharmaceutical Co., Ltd) for providing TAS-103 and TAS-1-3383, and Darren Kok for assistance in writing this manuscript.

MOL #43307

### References

- Azuma R and Urakawa A (1997) Simultaneous determination of a novel anticancer drug, TAS-103, and its N-demethylated metabolite in monkey plasma by high-performance liquid chromatography using solid-phase extraction. *J Chromatogr B Biomed Sci Appl* **691**(1):179-185.
- Bacher G, Pool M and Dobberstein B (1999) The ribosome regulates the GTPase of the beta-subunit of the signal recognition particle receptor. *J Cell Biol* **146**(4):723-730.
- Byl JA, Fortune JM, Burden DA, Nitiss JL, Utsugi T, Yamada Y and Osheroff N (1999) DNA topoisomerases as targets for the anticancer drug TAS-103: primary cellular target and DNA cleavage enhancement. *Biochemistry* **38**(47):15573-15579.
- Chen CL, Fuscoe JC, Liu Q and Relling MV (1996) Etoposide causes illegitimate V(D)J recombination in human lymphoid leukemic cells. *Blood* **88**(6):2210-2218.
- Dean KA, von Ahsen O, Gorlich D and Fried HM (2001) Signal recognition particle protein 19 is imported into the nucleus by importin 8 (RanBP8) and transportin. *J Cell Sci* **114**(Pt 19):3479-3485.

MOL #43307

Dignam JD, Lebovitz RM and Roeder RG (1983) Accurate transcription initiation by RNA

polymerase II in a soluble extract from isolated mammalian nuclei. *Nucleic Acids Res*

**11**(5):1475-1489.

Fortune JM, Velea L, Graves DE, Utsugi T, Yamada Y and Osheroff N (1999) DNA topoisomerases

as targets for the anticancer drug TAS-103: DNA interactions and topoisomerase catalytic

inhibition. *Biochemistry* **38**(47):15580-15586.

Ishida K and Asao T (1999) Interaction of a novel antitumor agent TAS-103 with DNA. *Nucleic*

*Acids Symp Ser*(42):129-130.

Keenan RJ, Freymann DM, Stroud RM and Walter P (2001) The signal recognition particle. *Annu*

*Rev Biochem* **70**:755-775.

Lakkaraju AK, Luyet PP, Parone P, Falguieres T and Strub K (2007) Inefficient targeting to the

endoplasmic reticulum by the signal recognition particle elicits selective defects in post-ER

membrane trafficking. *Exp Cell Res* **313**(4):834-847.

Lutcke H (1995) Signal recognition particle (SRP), a ubiquitous initiator of protein translocation.

*Eur J Biochem* **228**(3):531-550.

MOL #43307

Lutcke H, Prehn S, Ashford AJ, Remus M, Frank R and Dobberstein B (1993) Assembly of the 68-

and 72-kD proteins of signal recognition particle with 7S RNA. *J Cell Biol* **121**(5):977-985.

Ohtsu Y, Ohba R, Imamura Y, Kobayashi M, Hatori H, Zenkoh T, Hatakeyama M, Manabe T, Hino

M, Yamaguchi Y, Kataoka K, Kawaguchi H, Watanabe H and Handa H (2005) Selective

ligand purification using high-performance affinity beads. *Anal Biochem* **338**(2):245-252.

Osheroff N (1989a) Biochemical basis for the interactions of type I and type II topoisomerases with

DNA. *Pharmacol Ther* **41**(1-2):223-241.

Osheroff N (1989b) Effect of antineoplastic agents on the DNA cleavage/religation reaction of

eukaryotic topoisomerase II: inhibition of DNA religation by etoposide. *Biochemistry*

**28**(15):6157-6160.

Politz JC, Yarovoi S, Kilroy SM, Gowda K, Zwieb C and Pederson T (2000) Signal recognition

particle components in the nucleolus. *Proc Natl Acad Sci U S A* **97**(1):55-60.

Rose-John S, Schooltink H, Schmitz-Van de Leur H, Mullberg J, Heinrich PC and Graeve L (1993)

Intracellular retention of interleukin-6 abrogates signaling. *J Biol Chem*

**268**(29):22084-22091.

MOL #43307

Rosenblad MA, Gorodkin J, Knudsen B, Zwieb C and Samuelsson T (2003) SRPDB: Signal

Recognition Particle Database. *Nucleic Acids Res* **31**(1):363-364.

Schabel FM, Jr., Trader MW, Laster WR, Jr., Corbett TH and Griswold DP, Jr. (1979)

cis-Dichlorodiammineplatinum(II): combination chemotherapy and cross-resistance studies with tumors of mice. *Cancer Treat Rep* **63**(9-10):1459-1473.

Shima D, Yugami M, Tatsuno M, Wada T, Yamaguchi Y and Handa H (2003) Mechanism of H-8

inhibition of cyclin-dependent kinase 9: study using inhibitor-immobilized matrices. *Genes Cells* **8**(3):215-223.

Shimizu N, Sugimoto K, Tang J, Nishi T, Sato I, Hiramoto M, Aizawa S, Hatakeyama M, Ohba R,

Hatori H, Yoshikawa T, Suzuki F, Oomori A, Tanaka H, Kawaguchi H, Watanabe H and Handa H (2000) High-performance affinity beads for identifying drug receptors. *Nat Biotechnol* **18**(8):877-881.

Sunami T, Nishio K, Kanzawa F, Fukuoka K, Kudoh S, Yoshikawa J and Saijo N (1999)

Combination effects of TAS-103, a novel dual topoisomerase I and II inhibitor, with other anticancer agents on human small cell lung cancer cells. *Cancer Chemother Pharmacol*



MOL #43307

**43**(5):394-401.

Suzuki T, Kimura A, Nagai R and Horikoshi M (2000) Regulation of interaction of the acetyltransferase region of p300 and the DNA-binding domain of Sp1 on and through DNA binding. *Genes Cells* **5**(1):29-41.

Takano H, Kohno K, Matsuo K, Matsuda T and Kuwano M (1992) DNA topoisomerase-targeting antitumor agents and drug resistance. *Anticancer Drugs* **3**(4):323-330.

Tomohiro T, Sawada Ji J, Sawa C, Nakura H, Yoshida S, Kodaka M, Hatakeyama M, Kawaguchi H, Handa H and Okuno H (2002) Total analysis and purification of cellular proteins binding to cisplatin-damaged DNA using submicron beads. *Bioconjug Chem* **13**(2):163-166.

Torigoe T, Izumi H, Wakasugi T, Niina I, Igarashi T, Yoshida T, Shibuya I, Chijiwa K, Matsuo K, Itoh H and Kohno K (2005) DNA topoisomerase II poison TAS-103 transactivates GC-box-dependent transcription via acetylation of Sp1. *J Biol Chem* **280**(2):1179-1185.

Uga H, Kuramori C, Ohta A, Tsuboi Y, Tanaka H, Hatakeyama M, Yamaguchi Y, Takahashi T, Kizaki M and Handa H (2006) A new mechanism of methotrexate action revealed by target screening with affinity beads. *Mol Pharmacol* **70**(5):1832-1839.

MOL #43307

Utsugi T, Aoyagi K, Asao T, Okazaki S, Aoyagi Y, Sano M, Wierzba K and Yamada Y (1997)

Antitumor activity of a novel quinoline derivative, TAS-103, with inhibitory effects on topoisomerases I and II. *Jpn J Cancer Res* **88**(10):992-1002.

Wada T, Takagi T, Yamaguchi Y, Ferdous A, Imai T, Hirose S, Sugimoto S, Yano K, Hartzog GA,

Winston F, Buratowski S and Handa H (1998) DSIF, a novel transcription elongation factor that regulates RNA polymerase II processivity, is composed of human Spt4 and Spt5 homologs. *Genes Dev* **12**(3):343-356.

Wada T, Watanabe H, Usuda Y and Handa H (1991) Different biological activities of the hetero- and

homodimers formed by the 47- and 43-kilodalton proteins of transcription factor ATF/E4TF3. *J Virol* **65**(2):557-564.

Wang JC (1985) DNA topoisomerases. *Annu Rev Biochem* **54**:665-697.

Willmore E, Frank AJ, Padget K, Tilby MJ and Austin CA (1998) Etoposide targets topoisomerase

I $\alpha$  and I $\beta$  in leukemic cells: isoform-specific cleavable complexes visualized and quantified in situ by a novel immunofluorescence technique. *Mol Pharmacol* **54**(1):78-85.

Xiao H, Hasegawa T and Isobe K (2000) p300 collaborates with Sp1 and Sp3 in p21(waf1/cip1)

MOL #43307

promoter activation induced by histone deacetylase inhibitor. *J Biol Chem*

**275**(2):1371-1376.

Zwieb C and Eichler J (2002) Getting on target: the archaeal signal recognition particle. *Archaea*

**1**(1):27-34.

MOL #43307

### **Footnotes**

This study was supported by Special Coordination Funds for Promoting Science and Technology from the Japan Science and Technology Agency and by 21st Century COE program and Global COE program from the Ministry of Education, Culture, Sports, Science, and Technology of Japan. This work was also supported by a grant for research and development projects in Cooperation with Academic Institution from the New Energy and Industrial Technology Development Organization (NEDO).

MOL #43307

### Legends for figures

**Figure 1 Structures of the chemical compounds and preparation of TAS-1-3383-fixed latex beads.** (A) TAS-103; (B) TAS-1-3383; (C) preparation of TAS-103-immobilized affinity latex beads.

TAS-1-3383, a newly synthesized derivative of TAS-103, was immobilized to SGNGDENC beads.

The coupling reaction was performed as described in the Materials and Methods.

**Figure 2 Affinity purification using TAS-1-3383-fixed beads.** (A) Identification of the TAS-1-3383-binding protein. HeLa cell nuclear extracts were subjected to affinity purification using TAS-1-3383-fixed latex beads (lanes 2, 3, and 4) and the latex beads alone as a control (lane 1). The eluted proteins were subjected to silver staining. The asterisk indicates the specific band eluted from the TAS-1-3383-fixed latex beads. (B) The eluted proteins (lanes 2, 3, 4, and 5) and nuclear extract (lane 1) were analyzed by western blotting with anti-SRP54 antibody. (C) The extracts treated with RNase A (lanes 1, 2) and non-treated extracts (lanes 3, 4) were subjected to affinity purification using the TAS-1-3383-fixed beads (lanes 2, 4) and latex beads alone (lanes 1, 3). The eluted fractions were analyzed by western blotting with anti-SRP54 antibody.

MOL #43307

**Figure 3 Effects of TAS-103 on the SRP complex.** (A) 293T cells alone and 293T cells treated with 10  $\mu$ M TAS-103 for 24 hours were lysed with 0.5% NP-40 lysis buffer. The lysates were subjected to Superose-6 gel filtration and 18 fractions were collected. Each fraction was analysed by western blotting with antibodies for SRP54, SRP68, SRP72, and  $\beta$ -actin as a control. (B) The intensities of SRP54 (left) and  $\beta$ -actin (right) in gel-filtration chromatography fractions were measured using the NIH Image-J freeware program. The X-axis is the fraction number and the Y-axis is the intensity.

**Figure 4 Effects of TAS-103 on the interactions between SRP54 and other subunits.** (A) pcDNA3-FLAG-HIS-SRP54 was transfected into 293T cells. The cells were incubated for 12 hours with or without 10  $\mu$ M TAS-103 and lysed in lysis buffer containing 0.5% NP-40. The lysates were treated with RNaseA (lanes 5, 6, 11, 12). Over-expressed FLAG-tagged SRP54 was immunoprecipitated using ANTI-FLAG<sup>®</sup>-M2 agarose beads and released from the beads using FLAG peptide. The eluted fractions were analyzed by western blotting with anti-SRP54, anti-SRP68,

MOL #43307

anti-SRP72, anti-SRP19, anti-SRP14, and anti- $\beta$ -actin antibodies (lanes 1-6). Whole-cell lysates were also analyzed with the antibodies (lanes 7-12). (B) 293T cells were treated with or without 1  $\mu$ M, 3  $\mu$ M, or 10  $\mu$ M of TAS-103 for 12 hours and the lysates were analyzed by western blotting.

**Figure 5 Effects of TAS-103 and knockdowns of SRP14 or SRP54 on the translocation of IL-6-FLAG.** (A) 293T cells were transfected with pcDNA3.1-IL-6-FLAG, followed by a medium change after 16 hours. The cells were cultured for another 8 hours in the presence (lanes 3-5) or absence (lane 2) of TAS-103. The cells and culture media were collected 24 hours after transfection. The lysates and culture media were immunoprecipitated and analyzed by western blotting. (B) 293T cells were transfected with pcDNA3.1-IL-6 $\Delta$ S-FLAG followed by a medium change after 12 hours. The cells were cultured for another 8 hours in the presence (lanes 3-5) or absence (lane 2) of TAS-103. The cells and culture media were collected 24 hours after transfection. The lysates and culture media were immunoprecipitated and analyzed by western blotting. (C) 293T cells were co-transfected with the plasmid pcDNA3.1-IL-6-FLAG and stealth RNAs containing a scrambled sequence (lane 2) or targeting SRP14 (lane 3) or SRP54 (lane 4). The cells and culture media were collected 48 hours after

MOL #43307

transfection. The lysates and culture media were immunoprecipitated and analyzed by western blotting.

(D) 293T cells were co-transfected with the plasmid pcDNA3.1-IL-6 $\Delta$ S-FLAG and stealth RNAs

containing a scrambled sequence (lane 2) or targeting SRP14 (lane 3) or SRP54 (lane 4). The cells and

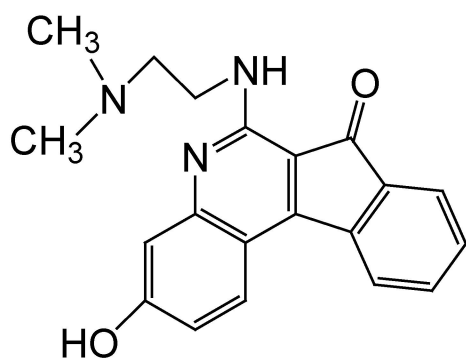
culture media were collected 48 hours after transfection. The lysates and culture media were

immunoprecipitated and analyzed by western blotting.



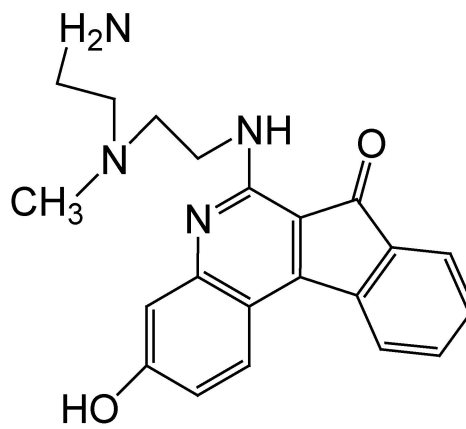
Figure 1

A



TAS-103

B



TAS-1-3383

C

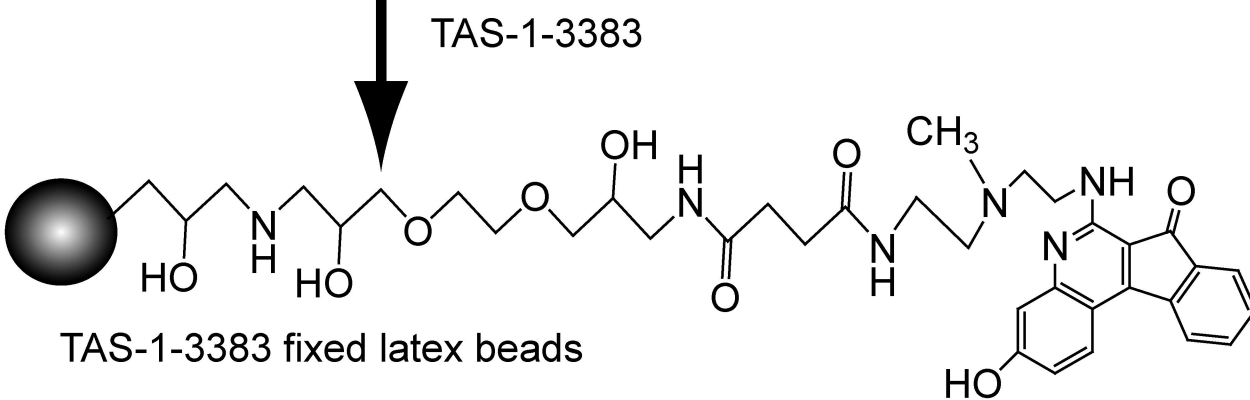
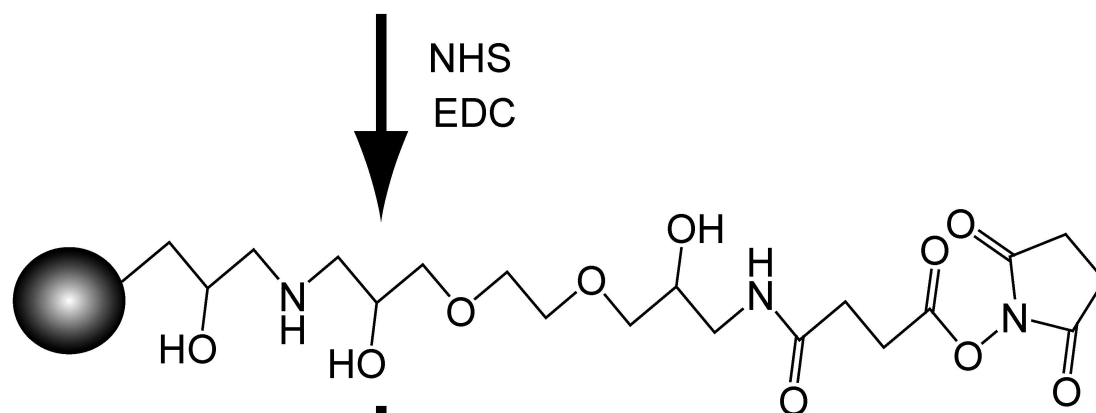
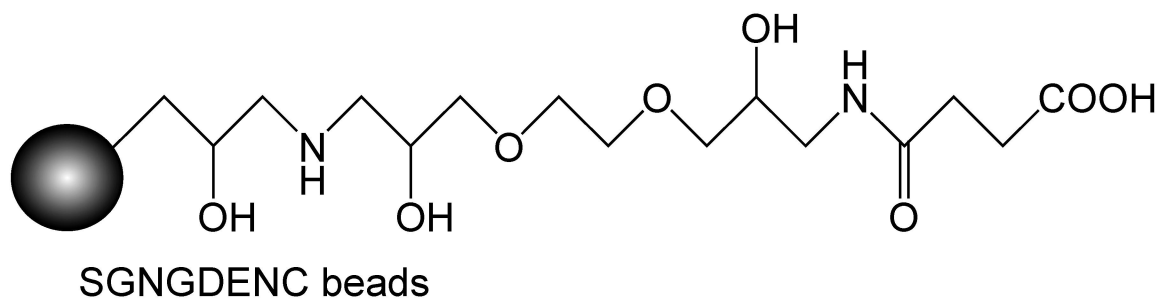
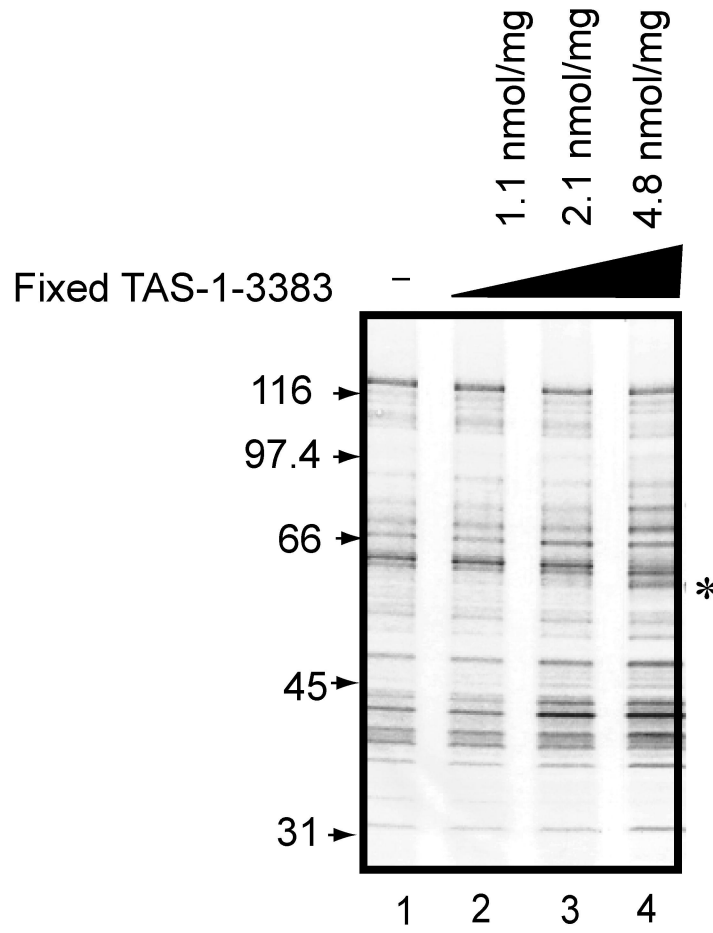
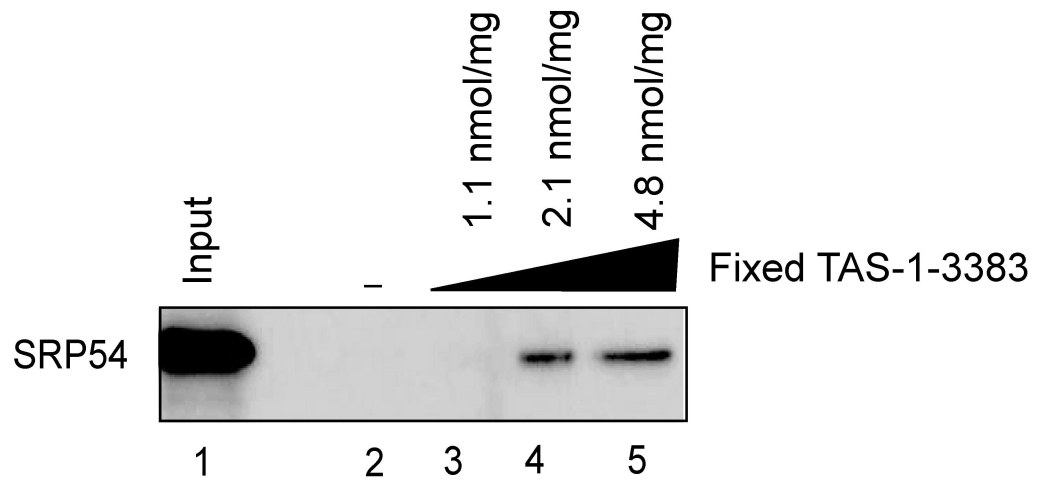


Figure 2

A



B



C

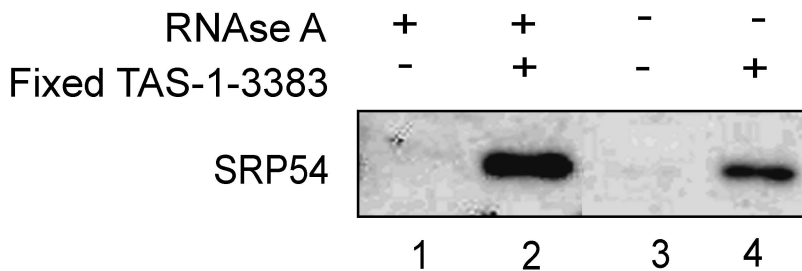


Figure 3

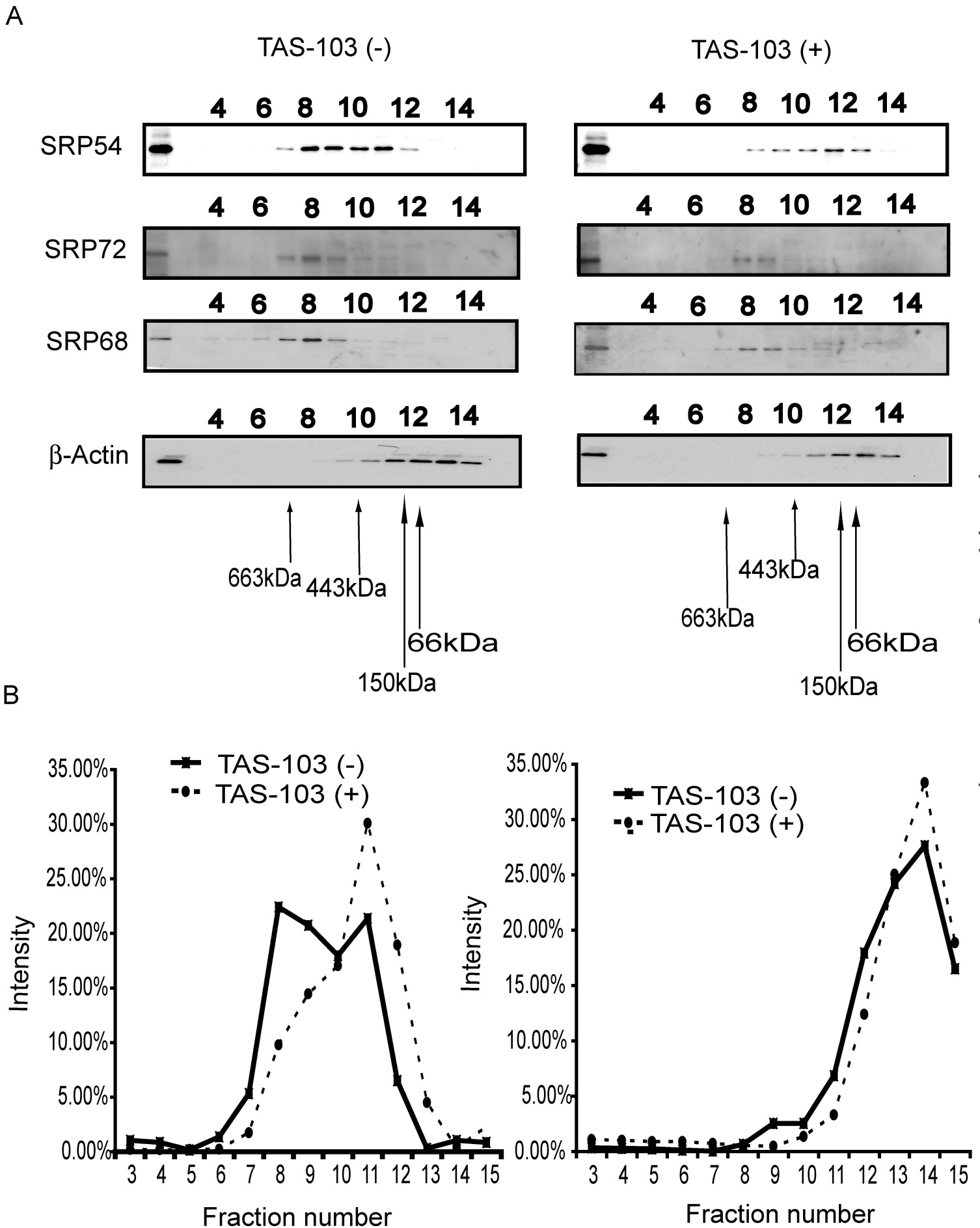
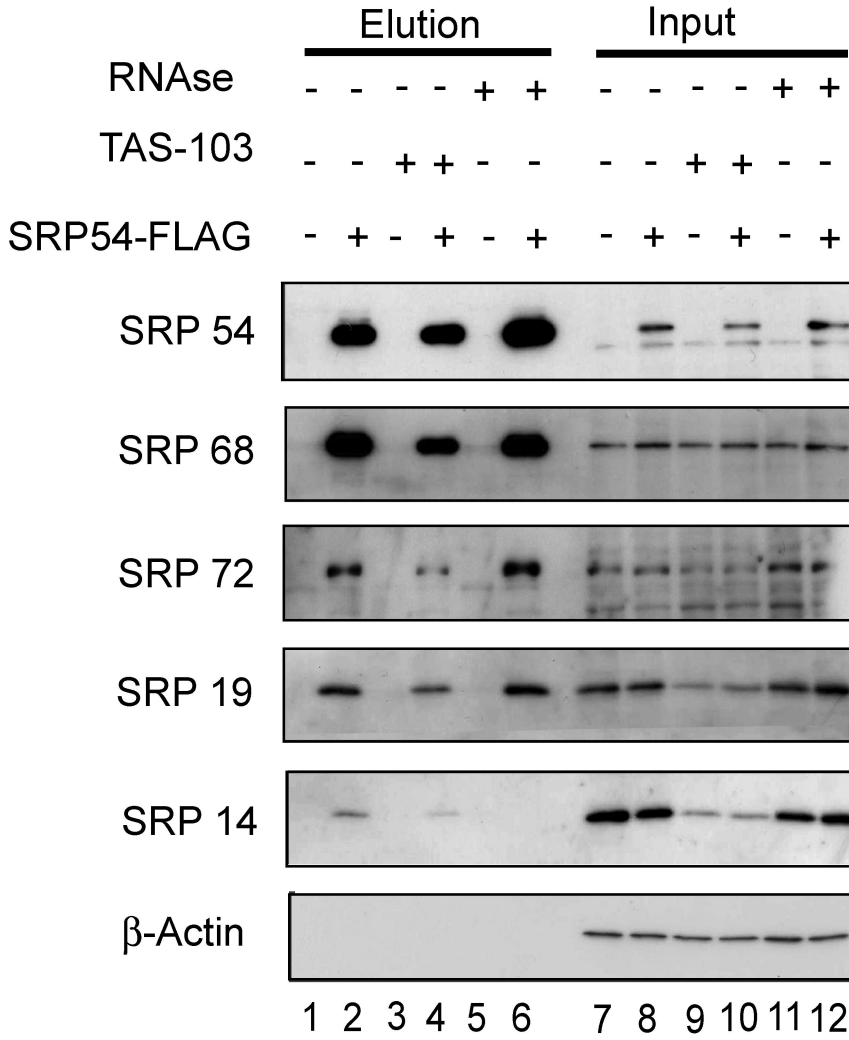


Figure 4

A



B

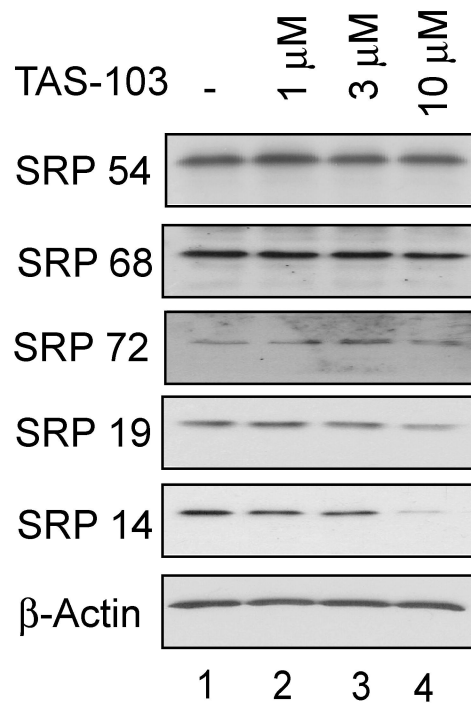


Figure 5

